Journal of Integrative Neuroscience

J. Integr. Neurosci. **2026**; 25(6): 52072
https://doi.org/10.31083/JIN52072

Original Research

Long-Term Effects of Early Postnatal Administration of R-Baclofen on Neuronal Properties in the *Cntnap2* Knockout Rat

Hannah Pineda[1], Susanne Schmid[1,2,*]

[1]Department of Anatomy & Cell Biology, University of Western Ontario, London, ON N6A 5C1, Canada
[2]Psychology Department, University of Western Ontario, London, ON, N6A 3K7, Canada
*Correspondence: Susanne.schmid@schulich.uwo.ca (Susanne Schmid)
Academic Editor: Woo-Yang Kim
Submitted: 20 March 2026 Revised: 22 April 2026 Accepted: 28 April 2026 Published: 12 June 2026

Abstract

Background: Contactin-associated protein-like 2 (*Cntnap2*) is a highly expressed gene during development, coding for the cell adhesion molecule CASPR2. Loss-of-function of *Cntnap2* leads to a neurodevelopmental disorder that presents with the core symptoms of autism. One prominent theory to explain autism symptoms is an imbalance of excitatory and inhibitory neurotransmitters, which leads to hyperexcitability in the autistic brain. R-baclofen, a γ-aminobutyric acid ($GABA_B$) receptor agonist, has been shown to acutely improve autism-like symptoms in rat models of autism, including exaggerated acoustic reactivity. However, the cellular basis and long-term impact of R-baclofen treatment during development are unknown. In the present study, we explored the impact of acute R-baclofen treatment on auditory cortical neurons and whether there are lasting changes in cell excitability and synaptic signaling following time-restricted R-baclofen administration during the critical period of auditory development. **Methods**: R-baclofen or saline were injected daily on postnatal days (PND) 14–21 and whole-cell patch clamp recordings were performed on pyramidal neurons in brain slices of the auditory cortex of juvenile (PND25–33) and adult (PND70–90) *Cntnap2* wild-type and knockout rats. **Results**: While acute R-baclofen application led to the expected reduction in cell excitability, early-life exposure to R-baclofen induced lasting changes in neuronal membrane properties and excitability. However, these effects were not uniformly beneficial, as in some instances they exacerbated the knockout phenotype and induced unwanted effects in wild-type neurons. **Conclusions**: The study shows that drug exposure in early age can change the developmental trajectory of the auditory system, indicating both opportunities and risks when considering early drug intervention.

Keywords: rat; autism; *Cntnap2*; sensory processing; R-baclofen; treatment

1. Introduction

Contactin-associated protein-like 2 (*CNTNAP2*) encodes the contactin-associated protein-like 2 (CASPR2) protein, which is a neurexin-family adhesion molecule predominantly expressed during development across sensory pathways, and plays a critical role in neuronal connectivity [1,2]. CASPR2 regulates neuronal excitability by clustering voltage-gated potassium channels at the juxtaparanodes of myelinated axons, synaptic terminals, and axonal segments [3,4,5,6,7]. *CNTNAP2* is highly conserved and expressed in humans and in animal models, including rodents [8]. Functional loss of *CNTNAP2* causes a syndromic disorder in humans, presenting with core symptoms of autism [9]. Accordingly, *Cntnap2* knockout (KO) rats express several autism-like traits—such as impaired social interactions, altered ultrasound vocalizations, hyperlocomotion, stereotypic movement, and altered auditory behaviour—making the *Cntnap2* KO rat a highly valid model for autism symptoms [1,10,11,12,13].

At the cellular level, *Cntnap2* KO disrupts excitatory and inhibitory (E/I) balance with reported abnormalities in dendritic spine morphology, AMPA (α-amino-3-hydroxy-5-methyl-4-isoxazolepropionic acid) receptor trafficking, inhibitory interneuron development, synaptic connectivity, and intrinsic neuronal excitability [14,15,16,17,18,19]. Recent work from our laboratory identified that *Cntnap2* KO phenotypes are also critically determined by developmental stage, with alterations in intrinsic excitability in cortical pyramidal neurons in the auditory cortex during the juvenile period followed by long-term changes in neurocircuits in adult synaptic networks [20].

A prominent theory of the neural basis for behavioural changes in autism spectrum disorder (ASD) posits an imbalance between the excitatory and inhibitory neurotransmitters (E/I balance), primarily involving glutamate and γ-aminobutyric acid (GABA) [21,22]. Post-mortem studies of individuals with autism have revealed altered glutamatergic signaling [23,24,25] and deficits in GABAergic signaling [26,27,28]. In accordance with this, we demonstrated that glutamine, glutamate and GABA are dysregulated in *Cntnap2* KO rats [29]. R-baclofen, a selective $GABA_B$ receptor agonist, has been discussed to potentially restore E/I balances in autism by enhancing inhibition. By activating presynaptic metabotropic GABA receptors, R-baclofen induces slow and prolonged inhibitory action by increasing outward potassium currents and inacti-

vating voltage-gated calcium channels [30]. Indeed, several studies indicate that acute administration of R-baclofen improves autism-related behaviours in various rodent models, including *Cntnap2* KO, such as social deficits, repetitive behaviours, cognitive deficits, and altered auditory processing [29,31,32,33]. Although these results seem encouraging, they were conducted predominantly in adult animals. In contrast, clinical trials with R-baclofen have been conducted predominantly in children and have yet to show convincing results [34,35], and were often hampered by methodological problems. Therefore, the long-term effects of R-baclofen administration during early childhood–a period of high brain plasticity–remain unclear. Building on our previous work on developmental changes in auditory cortical processing in *Cntnap2* KO rats, we here aim to further delineate when during development alterations occur, and how these changes are affected by early-life exposure to R-baclofen treatment. R-baclofen, or vehicle, was injected daily on postnatal days 14–21, a critical period for auditory system development shortly after the ear canals open and animals begin processing low-threshold auditory stimuli. This period is marked by a high level of activity-dependent synaptic plasticity [36,37,38,39]. Whole-cell patch-clamp recordings were performed on pyramidal neurons in the auditory cortex after cessation of treatment during a juvenile period and again in adulthood to assess the long-term effects of R-baclofen on membrane properties, intrinsic excitability, and synaptic input.

2. Materials and Methods

2.1 Animals

Male and female Sprague-Dawley *Cntnap2* wild-type (WT) and homozygous KO brain slices were obtained from litters bred through heterozygous *Cntnap2* crossing in our animal facility as described previously [13]. Briefly, original heterozygous *Cntnap2* breeders were obtained from Horizon Discovery (Boyertown; originally created at SAGE Laboratories, Inc.; the line is now maintained by Inotiv, PA, USA). Date of birth was assigned as postnatal day 0. Rats were genotyped via toe clipping at postnatal days (PND) 5–7 using polymerase chain reaction (PCR) and sequencing protocols as provided by the vendor. Experimental animals were used at two age ranges: postnatal day 25–33 (P25–33, juvenile) and postnatal day 70–90 (P70–90, adulthood). Animals were weaned on P21 and separated by sex before P35. Rats were housed in groups or pairs in a temperature-controlled room on a 12 h light/dark cycle with ad libitum food and water.

2.2 R-Baclofen Administration

R-baclofen was provided by the Simons Foundation for Autism Research free of cost. It was stored as a frozen concentrated stock solution that was diluted on each experimental day into 0.9% saline. Doses of 0.5 mg/kg were administered intraperitoneally daily, once a day, from postnatal days 14–21. Control animals received equal volumes of 0.9% saline.

2.3 Whole-Cell Patch Clamp Recordings

Sprague-Dawley WTs and homozygous *Cntnap2* KOs were anesthetized with 5% isoflurane (M60303, Fresenius Kabi Canada, Toronto, ON, Canada) and quickly decapitated for brain extraction. After removal, brains were rapidly placed into ice-cold slicing solution containing (in mM): 2.5 KCl, 1.25 NaH_2PO_4-H_2O, 24 $NaHCO_3$, 10 $MgSO_4$, 11 glucose, 234 sucrose, 2 $CaCl_2$, 3 Myoinositol, 2 Na-Pyruvate, and 0.4 ascorbate; saturated with 95% O_2/5% CO_2. Coronal slices of 300 µm containing the auditory cortex were cut using a vibrating microtome (Compresstome VF-200, Precisionary, Ashland, MA, USA) in a chamber filled with ice-cold slicing solution and then transferred into another holding chamber filled with artificial cerebrospinal fluid (ACSF) containing (in mM): 3 KCl, 1.25 NaH_2PO_4-H_2O, 3 $MgSO_4$, 26 $NaHCO_3$, 124 NaCl, and 10 glucose; saturation with 95% O_2/5% CO_2. $CaCl_2$ (2 mM) was added to the ACSF just before slices were transferred. Juvenile slices were left to rest for one hour at room temperature before recordings took place, while adult slices were placed in ACSF heated to ~35 °C for 30–40 minutes, and then left for an additional hour to rest at room temperature. Slices were kept at room temperature for the time of the experiment.

Electrophysiological experiments were performed as reported previously [20,40]. Briefly, whole- cell patch clamp recordings were taken from visually identified pyramidal neurons in layers 2/3 throughout the auditory cortex using an upright microscope (Zeiss Axioskop, Oberkochen, Germany), attached with an EMCCD camera (Evolve 512, Photometric, Tucson, AZ, USA). Patch pipettes were pulled on a P-97 Puller (Sutter Instrument, Novato, CA, USA) using fabricated borosilicate glass capillaries (1B150F-4, OD: 1.50 mm, ID: 0.84 mm, World Precision Instruments, Sarasota, FL, USA) and had resistances from 3–7 MΩ when filled with a filtered intracellular solution containing the following (in mM): 140 K-gluconate, 10 KCl, 1 $MgCl_2$, 10 HEPES, 0.02 EGTA, 3 Mg-ATP, and 0.5 Na-GTP, pH adjusted to 7.2–7.3, 290–300 mosmol. Signals were sampled at 10 kHz and amplified with Axopatch 200B (Axon Instruments, Molecular Devices, Sunnyvale, CA, USA), digitized with Digidata1550 (Axon Instruments), and analyzed using pClamp10.4 (Axon Instruments). Pyramidal cells with an access resistance >25 MΩ were discarded for analyses; parameters were continuously monitored throughout recordings. Pipette capacitance was compensated, access resistance and cell capacitance were not compensated. Junction potential was calculated to be +15 mV using the Nernst-Planck equation via LJPcalc software (https://swharden.com/LJPcalc; [27]) and was not compensated for.

Voltage-clamp membrane test using 10-mV step was used to assess cell capacitance and membrane resistance.

The membrane potential was held at –70 mV for all voltage-clamp recordings. Resting membrane potentials (RMPs) were measured in current-clamp while holding the current at I = 0. Current-clamp recordings using 40 pA steps to measure action potential features including firing threshold, half-widths, rheobase current, and firing frequencies were made while adjusting the current to keep the cells at –70 mV, as described prior [20].

For acute administration of R-baclofen on brain slices at P14, R-baclofen was added to the bath solution (N = 2 rats, n = 7 cells). Once whole-cell was achieved, current clamp recordings to measure action potentials were taken under control conditions while adjusting current to keep cells' membrane potential at –70 mV, which was close to their resting membrane potentials (RMP). 1-s long step current injections in 40 pA increments from –120 pA to +440 pA took place to assess rheobase and firing frequencies. Subsequently, R-baclofen was perfused with the bath, and current-clamp recordings were taken after 3–5 minutes of wash-in.

Spontaneous postsynaptic currents (sPSCs) were assessed in voltage-clamp with 5-minute recordings of cell currents while holding the cells at –70 mV. For recording evoked postsynaptic currents (ePSC), layers 5/6 of the auditory cortex were stimulated using a bipolar tungsten electrode (Science Products, Hofheim, Germany) and paired pulses were generated with a pulse generator (Master-8, AMPI, Jerusalem, Israel). This stimulation likely activates multiple synapses, including inputs from layers 5/6 neurons and axons in surrounding areas, and from neurons in layer 2/3 [20]. Paired pulse ratios (PPR) were calculated using an interstimulus interval of 50 ms.

2.4 Offline Analysis

Passive membrane properties (RMP, membrane capacitance, membrane resistance), current clamp step recordings, and ePSCs were analyzed in pClamp10.4 (Molecular Devices, San Jose, CA, USA). Action potential threshold was considered to be the baseline voltage of the first action potential, while rheobase was the accompanying current that elicited the first action potential. Action potential half-width was recorded from the second spike elicited from the rheobase current, measured as the width (ms) of that event's half amplitude. Firing frequencies were found by manually counting the number of spikes elicited during the 1s of each step current injection. Paired pulse ratio for ePSCs were calculated as the amplitude of the second ePSC divided by the amplitude of the first. The amplitude and frequencies of sPSCs were analyzed in MiniAnalysis (v.6.0.8., Synaptosoft, Fort Lee, NJ, USA). A minimum amplitude of 5 pA was set as criteria. Data analyses were performed with pClamp10.4 (Molecular Devices), and/or Microsoft Excel 2016 (Microsoft Corp., Redmond, WA, USA). Groups sizes (N = animal/n = recorded cells) were as follows: P25–33: saline-WT: N = 5–6/n = 9–13 (1–4 cells per animal); saline-KO: N = 5–7/n = 9–12 (1–5 cells per animal); R-baclofen (rbac)-WT: N = 4–5/n = 10–12 (1–5 cells per animal); rbac-KO: N = 4–7/n = 10–12 (1–6 cells per animal). P70–90: saline-WT: N = 3/n = 9–11 (1–4 cells per animal); saline-KO: N = 3/n = 8–9 (1–4 cells per animal); rbac-WT: N = 4/n = 9–10 (1–4 cells per animal); rbac-KO: N = 5/n = 8–10 (1–3 cells per animal).

2.5 Data Presentation and Statistics

Graphs were generated with GraphPad (Prism 10.4.1 for Windows, GraphPad Software, San Diego, CA, USA). Sample recordings were created in pClamp. Statistical analyses were conducted using R Studio (v.2025.05.0+496; Posit Software, PBC, Boston, MA, USA). All data was analyzed using linear mixed-effects models using the lme4 package (https://cran.r-project.org/web/packages/lme4/index.html) to account for repeated measurements within cells (firing frequencies) and for hierarchal structure of the data, specifically that multiple cells were recorded per animal (cells nested within animals). The statistical analysis of fixed effects was determined with Type II Analysis of Variance with Satterthwaite's approximation for degrees of freedom (lmerTest package, https://cran.r-project.org/web/packages/lmerTest/index.html). Type II was preferred due to unequal distribution of cells per animal across groups and its compatibility with mixed models. Model assumptions were assessed by visual inspection of residuals using Q–Q plots, as normality assumptions in linear mixed models pertain to model residuals rather than raw data. When significant interactions were detected, we conducted post hoc simple effects analyses using estimated marginal means and Tukey adjustment to compare genotypes within treatments and treatments within genotypes (emmeans package, https://cran.r-project.org/web/packages/emmeans/index.html). Outlier detection was performed in GraphPad. Outliers identified by this procedure were excluded using the ROUT method with Q = 1%, in order to remove values that were statistically flagged as inconsistent with the overall distribution while limiting the expected proportion of false-positive exclusions to 1%. As such, outliers were removed in the following measures: P25–33 firing threshold (2 cells, both WT-sal), P25–33 sPSC frequency (1 cell, WT-sal), P70–90 capacitance (1 cell, WT-rbac), and P70–90 membrane resistance (2 cells, 1 KO-sal and 1 WT-rbac). If cell health was questioned during a recording it was discarded and excluded from analysis, for example, if membrane potential became unstable during sPSC recordings or if a cell could not be evoked for PPR analysis. Statistically significant differences were determined as p values being less than $\alpha = 0.05$. Exact p-values are reported, unless $p < 0.001$. Male and female animals were analyzed together to maximize statistical power, since sample sizes within each sex were not sufficient to support reliable analyses of sex-specific effects. As well, the distribution of males and females was not balanced across experi-

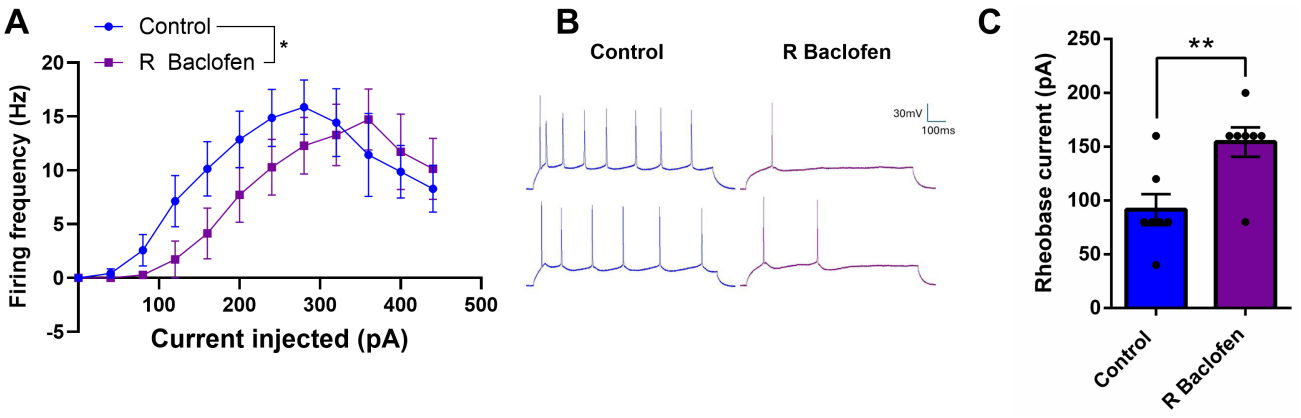

Fig. 1. Acute perfusion with R-baclofen reduces excitability of auditory neurons at P14. (A) Firing frequencies before and after R-baclofen administration in response to increasing current stimuli. Graph shows mean ± SEM. (B) Sample traces of action potential trains in response to a 160 pA current. (C) Rheobase current of auditory cortical neurons is significantly increased after perfusion with R-baclofen in acute brain slices. Animal/cell counts: N = 2/n = 7. Graph shows mean ± SEM. Statistical comparisons were performed using a linear mixed-effects model. Asterisks indicate significant differences, *$p < 0.05$, **$p < 0.01$.

mental groups, restricting the ability to appropriately model sex as an independent factor. This limiting factor is elaborated on in the discussion as a limitation.

3. Results

3.1 Inhibitory Effect of Acute R-Baclofen Administration in Auditory Cortical Neurons

To first establish the effect of acute R-baclofen administration, we measured the excitability of auditory cortical neurons by evaluating firing frequency and rheobase current before and after perfusion with 10 µM R-baclofen (Fig. 1) in slices at P14. Firing frequency was significantly reduced by R-baclofen application ($F_{(1, 158)} = 6.229$, $p = 0.014$, Fig. 1A,B). Furthermore, rheobase current significantly increased following R-baclofen perfusion ($F_{(1, 11)} = 14.61$, $p = 0.003$). Taken together, the lower firing frequency in response to current stimulation and increased rheobase current identify an inhibitory effect of acute R-baclofen.

3.2 Age Dependent Differences in Passive Membrane Properties Mediated by Genotype and R-Baclofen Treatment

Next, we evaluated the long-term impact of R-baclofen treatment during the critical period on passive membrane properties in juvenile and adult *Cntnap2* KO and WT rats. In juvenile animals, analysis of resting membrane potential (RMP) revealed a genotype x treatment interaction ($F_{(1, 22.179)} = 4.6077$, $p = 0.043$; Fig. 2A). Post hoc Tukey tests indicated significantly more negative RMPs in neurons from saline-treated KO animals compared to saline-treated WT ($p = 0.018$). Interestingly, neurons from R-baclofen-treated WT rats also showed lower RMPs than saline-treated WT ($p = 0.0456$), in which the treatment made them more similar to the KO groups. R-baclofen treatment had no effect on RMPs in *Cntnap2* KO rats ($p = 0.427$). In brain slices from adult animals, there were no longer any significant effects of either genotype or treatment on RMP (Fig. 2B).

In terms of cell capacitance, there were no significant effects of either genotype or treatment across any age range (Fig. 2C,D). Analysis of juvenile membrane resistance also demonstrated no genotypic or treatment effects, whereas adults exhibited a trend of genotype ($F_{(1, 34)} = 3.7434$, $p = 0.0614$) and a trend towards a genotype × treatment interaction ($F_{(1, 34)} = 3.9219$, $p = 0.0558$) (Fig. 2E,F).

3.3 Action Potential Features are Unaffected by Genotype and Treatment Across Development

To further evaluate long-term effects of prior R-baclofen treatment, we assessed action potential features in auditory cortical neurons elicited by current stimulation (Fig. 3A–G). While there were no main effects of genotype or treatment, there was a trend towards an interaction between treatment × genotype in animals aged P25–33 ($F_{(1, 10.687)} = 4.493$, $p = 0.0583$) for firing thresholds (Fig. 3B). No main effects, nor interactions, were observed in adulthood (Fig. 3C). Analysis of rheobase current also showed no effect of treatment, genotype, or interactions for either age (Fig. 3D,E). Similarly, analysis of action potential half-widths revealed no effects or interactions during the juvenile or adult stage (Fig. 3F,G).

3.4 R-Baclofen Treatment Induces Alterations in Firing Frequency That Persist Into Adulthood

We subsequently examined firing frequency patterns in the current-clamp mode. At P25–33, there were no main effects of genotype or treatment, but there was a significant effect of current ($F_{(1, 469)} = 2830.083$, $p < 0.001$) and an interaction between current and treatment ($F_{(1, 469)} = 9.901$,

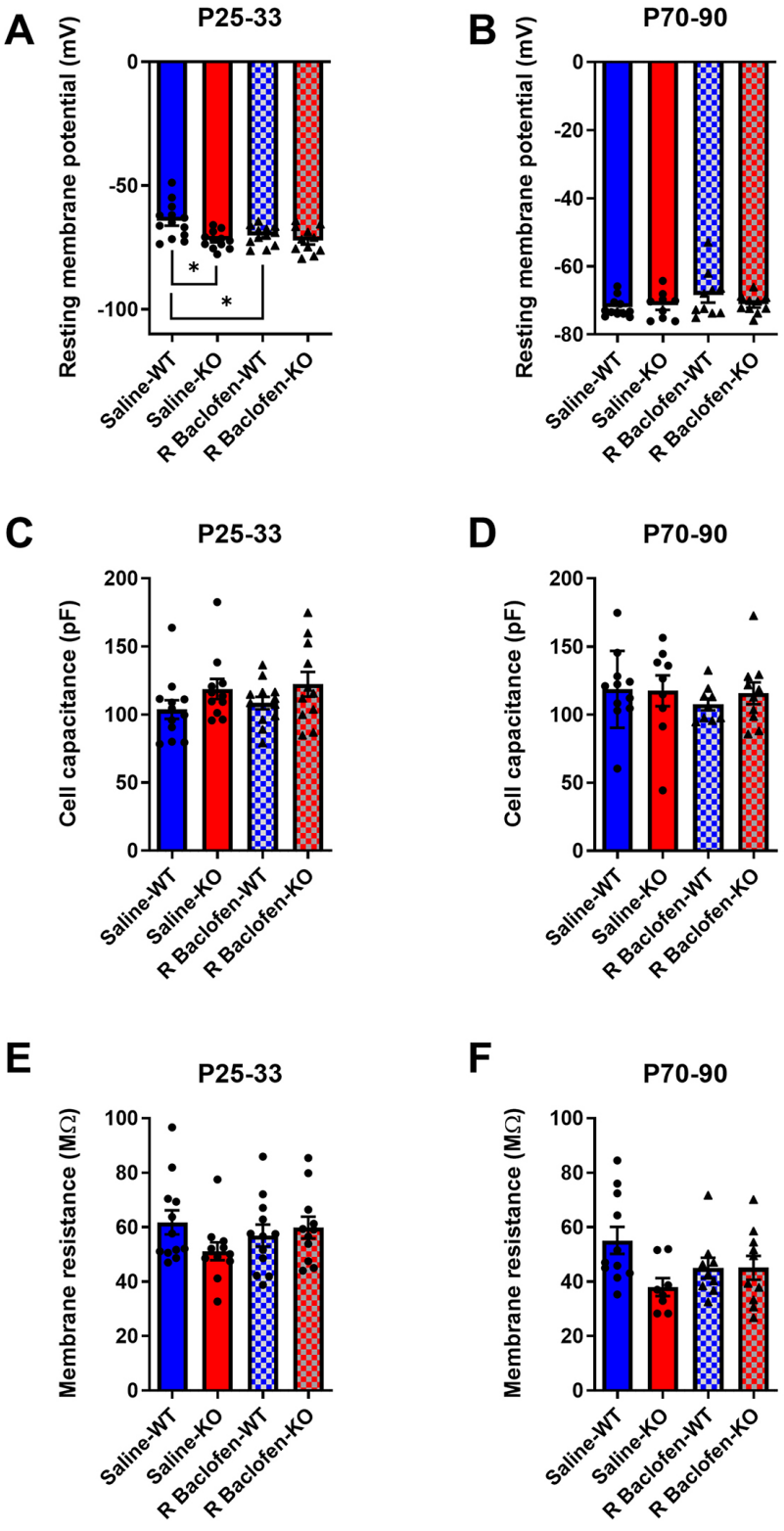

Fig. 2. Passive membrane properties are changed by R-baclofen depending on genotype and age. (A,B) Resting membrane potential, (C,D) cell capacitance, (E,F) and membrane resistance of auditory cortical pyramidal neurons in wild type (WT) and contactin-associated protein-like 2 (*Cntnap2*) knockout (KO) rats that were treated from P14–P21 with R-baclofen or vehicle. Animal/cell counts–P25–33: saline-WT: N = 6/n =12–13, saline-KO: N = 7/n = 11–12, R-baclofen (rbac)-WT: N = 5/n = 12, rbac-KO: N = 6–7/n = 11; P70–90: saline-WT: N = 3/n = 11, saline-KO: N = 3/n = 9, rbac-WT: N = 4/n = 10, rbac-KO: N = 5/n = 10. Graphs show means ± SEM. Statistical comparisons were performed using a linear mixed-effects model. Asterisks indicate significant differences, *$p < 0.05$. WT, *Cntnap2* wild-type; KO, *Cntnap2* knockout.

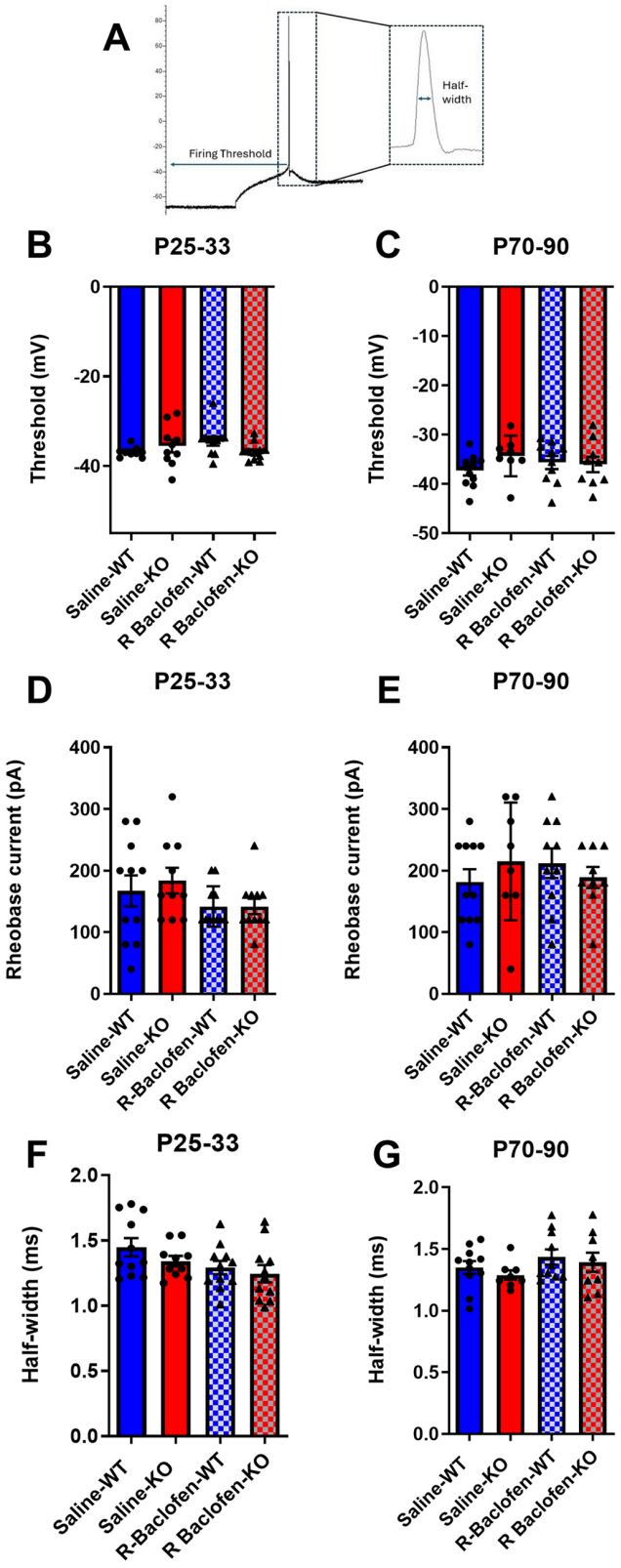

Fig. 3. Action potential features. (A) Sample current clamp recording indicating firing threshold and half-width. (B,C) Firing thresholds, (D,E) rheobase current amplitudes, (F,G) action potential half-widths in brain slices from juvenile and adult *Cntnap2* KO and WT animals treated with saline or R-baclofen from P14–21. Animal/cell counts–P25–33: saline-WT: N = 6/n = 11, saline-KO: N = 5/n = 10, rbac-WT: N = 5/n = 11, rbac-KO: N = 5/n = 11; P70–90: saline WT: N = 3/n = 11, saline-KO: N = 3/n = 8, rbac-WT: N = 4/n = 10, rbac-KO: N = 5/n = 9. Statistical comparisons were performed using a linear mixed-effects model. Graphs show means ± SEM.

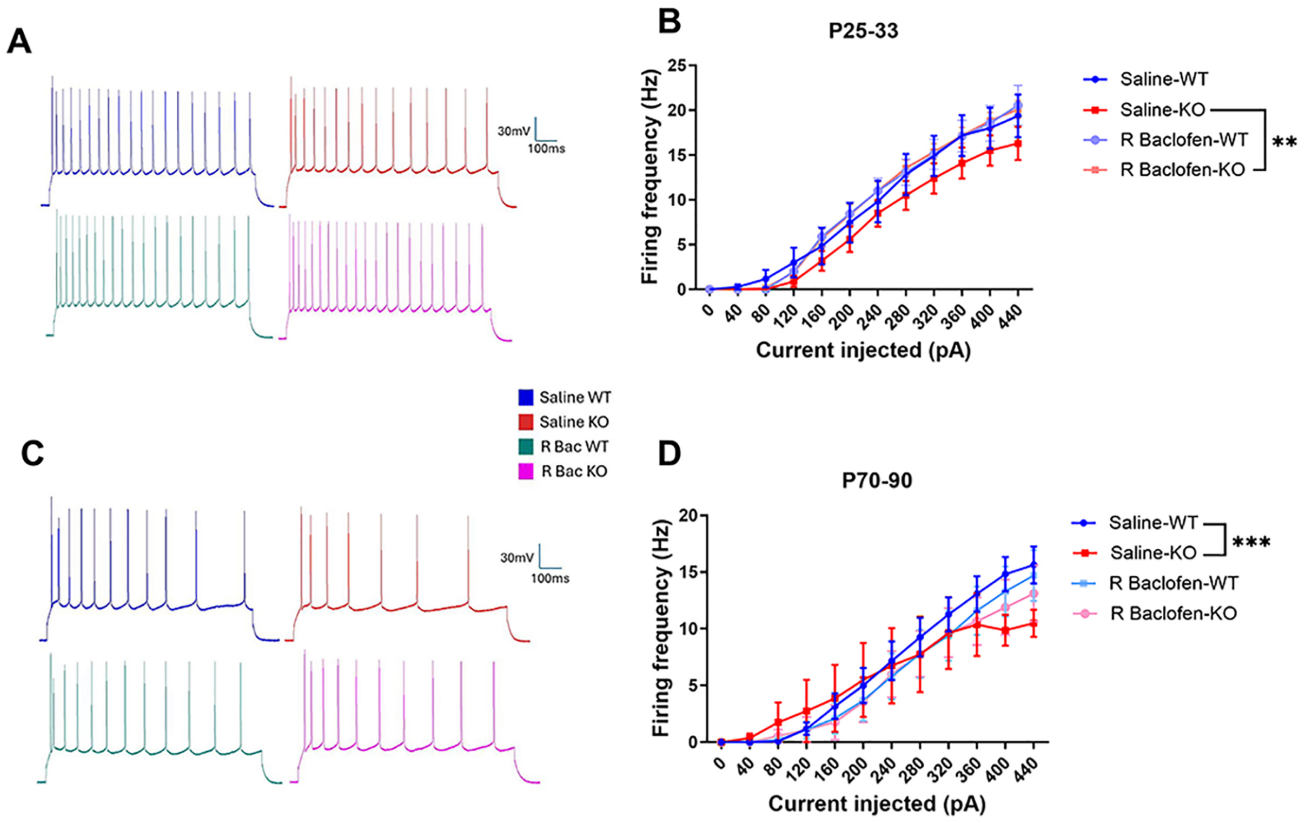

Fig. 4. Firing frequencies during juvenile (P25–33) and adult (P70–90) age ranges comparing genotype and treatment. (A,C) sample recordings from each group at +440 pA current injection. (B,D) F-I curves for juvenile and adult rats treated with saline or R-baclofen. Animal/cell counts–P25–33: saline-WT: N = 6/n = 11, saline-KO: N = 5/n = 10, rbac-WT: N = 5/n = 11, rbac-KO: N = 5/n = 11; P70–90: saline WT: N = 3/n = 11, saline-KO: N = 3/n = 8, rbac-WT: N = 4/n = 10, rbac-KO: N = 5/n = 9. Graphs depict mean ± SEM. Statistical comparisons were performed using a linear mixed-effects model. Asterisk indicates significant differences between F-I slopes, $^{**}p < 0.01$, $^{***}p < 0.001$.

$p = 0.002$; Fig. 4A,B). Post hoc Tukey tests did not detect significant differences between treatment groups at individual current steps; however, pairwise comparisons of the frequency-current (F-I) curve indicated that R-baclofen altered the input-output function in KO neurons. Specifically, the F-I slope in R-baclofen-treated KOs was significantly steeper than in saline-treated KOs ($p = 0.005$). Notably, R-baclofen-treated KOs fired similarly to saline-WTs ($p = 0.702$), whereas saline-KOs trended to fire at lower rates compared to saline-WTs ($p = 0.098$). At P70–90, there was a significant main effect of current ($F_{(1, 414)} = 1024.252$, $p < 0.0001$), significant interactions of current × genotype ($F_{(1, 414)} = 15.594$, $p < 0.0001$) and current × genotype × treatment ($F_{(1, 414)} = 6.081$, $p = 0.014$; Fig. 4C,D). Post hoc comparisons again indicated no statistical differences between genotypes, or genotype × treatment combinations at individual current steps. Nonetheless, pairwise slope comparisons revealed a marked divergence between KO-saline and WT-saline groups ($p < 0.0001$). Treatment with R-baclofen in KO neurons attenuated this difference, such that the comparison with WT-saline was no longer statistically significant ($p = 0.076$).

3.5 R-Baclofen Administration Increases Synaptic Input During P25–33

In order to determine the long-term effect of R-baclofen administration during the critical period on synaptic input on auditory cortical neurons in the *Cntnap2* KO rat, we measured spontaneous postsynaptic currents (sPSCs, Fig. 5A,B). During the juvenile age range, there were no effects or interactions on sPSC amplitude (Fig. 5C). However, sPSC frequencies increased due to a main effect of genotype ($F_{(1, 11.077)} = 9.678$, $p = 0.0098$) and main effect of treatment ($F_{(1, 11.280)} = 4.935$, $p = 0.048$; Fig. 5D). Post hoc analysis revealed that this effect was driven by R-baclofen-treated KOs, which showed significantly higher frequencies compared to saline-treated KOs ($p = 0.047$) and R-baclofen-treated WTs ($p = 0.025$). In adulthood, there were no more significant main effects present for either amplitude or frequency of sPSCs (sPSC frequency: genotype–$p = 0.418$, treatment–$p = 0.169$; sPSC amplitude: genotype–$p = 0.589$, treatment–$p = 0.367$) (Fig. 5E,F).

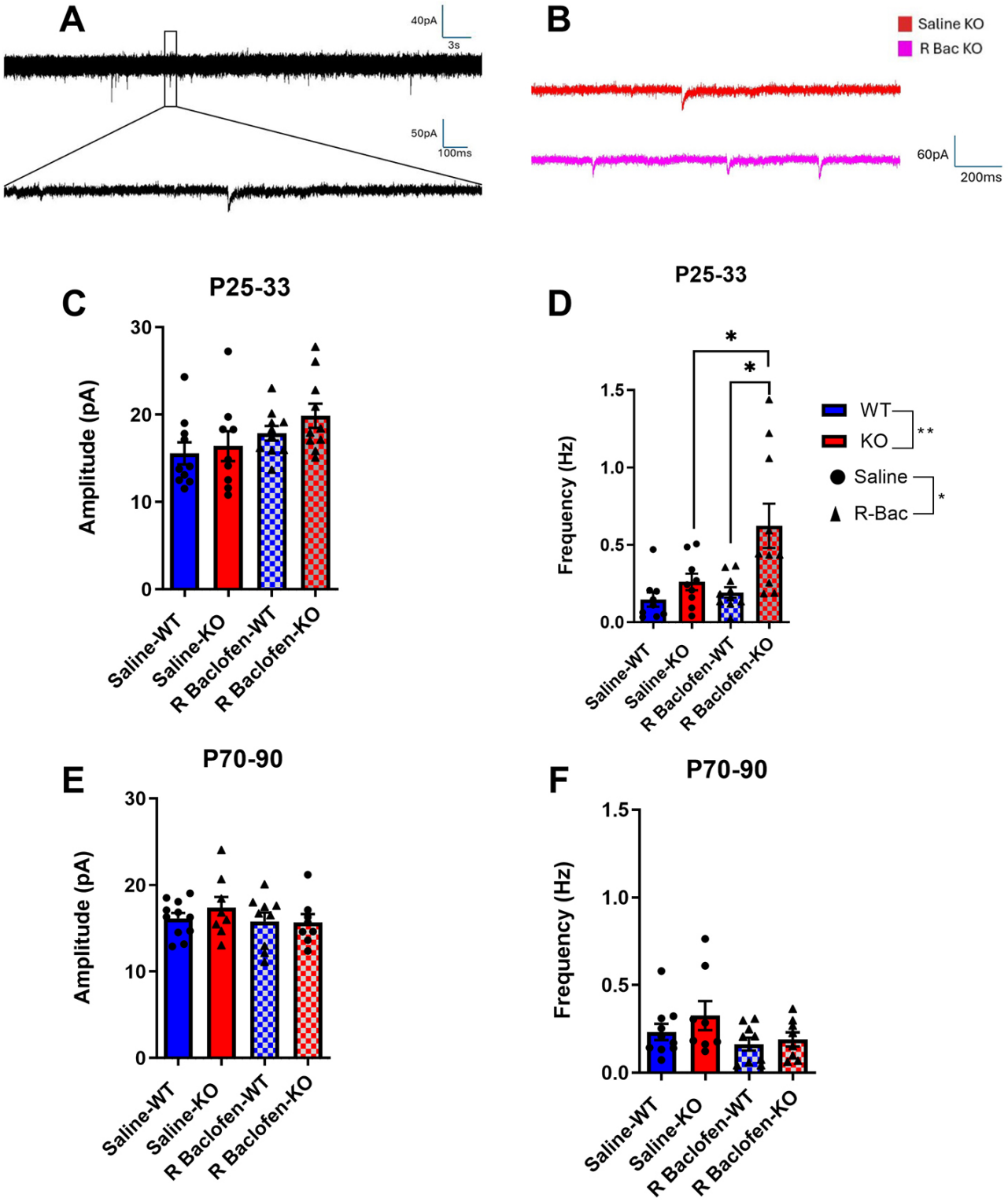

Fig. 5. Spontaneous postsynaptic currents (sPSCs) are affected by treatment and genotype during juvenile age, but not during adulthood. Sample recording of sPSCs (A,B). Amplitude and frequency of sPSCs in *Cntnap2* KO and WT rats treated with saline or R-baclofen during juvenile age range (C,D) and adulthood (E,F). Animal/cell counts–P25–33: saline-WT: N = 5/n = 9–10, saline-KO: N = 5/n = 9, rbac-WT: N = 5/n = 10, rbac-KO: N = 5/n = 10; P70–90: saline WT: N = 3/n = 10, saline-KO: N = 3/n = 8, rbac-WT: N = 4/n = 9, rbac-KO: N = 5/n = 8. Graphs show means ± SEM. Statistical comparisons were performed using a linear mixed-effects model. Asterisk indicates significant differences, $*p < 0.05$, $**p < 0.01$.

3.6 Synaptic Release Probabilities are not Changed After R-Baclofen Treatment

Paired pulse evoked PSCs were elicited by stimulating in the pyramidal neuron layers 5/6 of the auditory cortex to assess presynaptic release probability in the *Cntnap2* KO rat, and to see if this is impacted by R-baclofen treatment. During P25–33, KO animals exhibited significantly higher PPR values than WT animals, indicating a lower release probability (main effect of genotype: $F_{(1, 9.9043)} = 9.7375$, $p = 0.011$; Fig. 6A,C). By adulthood, this effect of genotype was no longer apparent ($p = 0.624$; Fig. 6B,D). R-baclofen treatment did not have any significant effects at either age range (juvenile: $p = 0.747$, adult: $p = 0.751$).

4. Discussion

The present study examined the acute and long-term effects of R-baclofen administration early in development on electrophysiological properties of neurons in the auditory cortex in *Cntnap2* WT and KO rats. We have previously shown that acute administration of R-baclofen ameliorates characteristic changes in brainstem-mediated auditory behaviour in *Cntnap2* KO rats, i.e., it reduces exaggerated startle responses and reverses the much lower startle thresholds in KO animals [29]. Building on this, the goal of the current study was to show both the acute effect of R-baclofen on neuronal signaling in the auditory cortex and to also evaluate the long-term effects of early R-baclofen administration during development on auditory processing, which is a more clinically-relevant paradigm given that clinical treatment trials include mostly children.

4.1 Acute R-Baclofen Administration

Acute bath administration of R-baclofen at P14 induced the expected generally inhibitory effect in auditory cortical neurons, evidenced by increased rheobase and decreased firing frequency at moderate current injections. Firing partially recovered when neurons were strongly depolarized with high depolarizing current injections, indicating a downward and rightward shift of the F-I curve. This aligns with known mechanistic effects of R-baclofen: increased activation of pre- and post-synaptic $GABA_B$ receptors inhibits voltage-gated calcium channels [41,42] and opens protein-coupled inwardly rectifying potassium (GIRK) channels [43], collectively reducing excitability during current stimulation. Others have also identified potent and dose-dependent effects of R-baclofen on firing frequencies, with high concentrations or additional cofactors often achieving full suppression of neuronal activity [44,45]. Although cortical auditory neurons are not directly involved in mediating acoustic startle responses [46], it can be presumed that similar inhibitory effects on auditory brainstem startle neurons are responsible for reversing higher startle responses in *Cntnap2* KO rats.

4.2 Effects of Early Treatment With R-Baclofen on Cell Properties

To determine any long-term effect of R-baclofen on neuronal properties, we injected animals for eight consecutive days during a critical period for auditory development (P14–21), when the meatus has opened and low threshold auditory information is reaching the brain, coinciding with a phase of high activity-dependent plasticity and synaptic re-organization [37,47]. We evaluated changes in electrophysiological properties in the auditory cortex in juvenile (P25–33) and adult (P70–90) neurons. This approach allowed us to identify potential long-term consequences of early-life exposure to R-baclofen during the critical period.

Passive membrane properties were not different between *Cntnap2* KO and wildtype rats in neither juvenile nor adults, with the exception of a slightly more negative resting membrane potential in juvenile *Cntnap2* KO neurons. While genotypic changes in resting membrane potentials have been described in fast-spiking *Cntnap2* KO interneurons within the somatosensory cortex of mice [17], our prior investigation found no major differences in passive membrane properties between *Cntnap2* KO and WT pyramidal neurons; however it did show notable developmental changes between P8 and P18, and no developmental changes thereafter [20]. It is important to note that the difference in RMP observed in neurons from juvenile WT versus KO animals is in the same direction as these rapid developmental changes occurring just before the juvenile stage analysed here [20]. As such, we cannot entirely exclude the possibility that slices from KOs were taken from animals more towards the older limit of the juvenile age range, while slices from WT animals might have been taken more towards the younger limit, which could explain these slight differences and the fact that we didn't observe them in the previous study [20]. Interestingly, our results also show that in juvenile animals treated with R-baclofen, the resting membrane potentials in WT neurons no longer different from *Cntnap2* KO saline and R-baclofen-treated neurons, indicating that if anything, R-baclofen may have produced unwanted effects in juvenile WT animals but no effect in KO animals or on passive membrane properties in the adult stage of either genotype.

Action potential features, including firing threshold, half-width, and rheobase, were not significantly altered by genotype at either age examined here. We previously reported reduced rheobase and action potential half-width in *Cntnap2* KO auditory neurons at P18–21, a critical developmental period when neurons and their networks are still maturing in rats. These differences are normalized by adulthood [20]. The later juvenile stage examined in the present study (P25–33 as opposed to P18–21 in the previous study) indicates that these genotypic differences start to converge as early as P21–25. R-baclofen treatment did not have any long-term effect on action potential features.

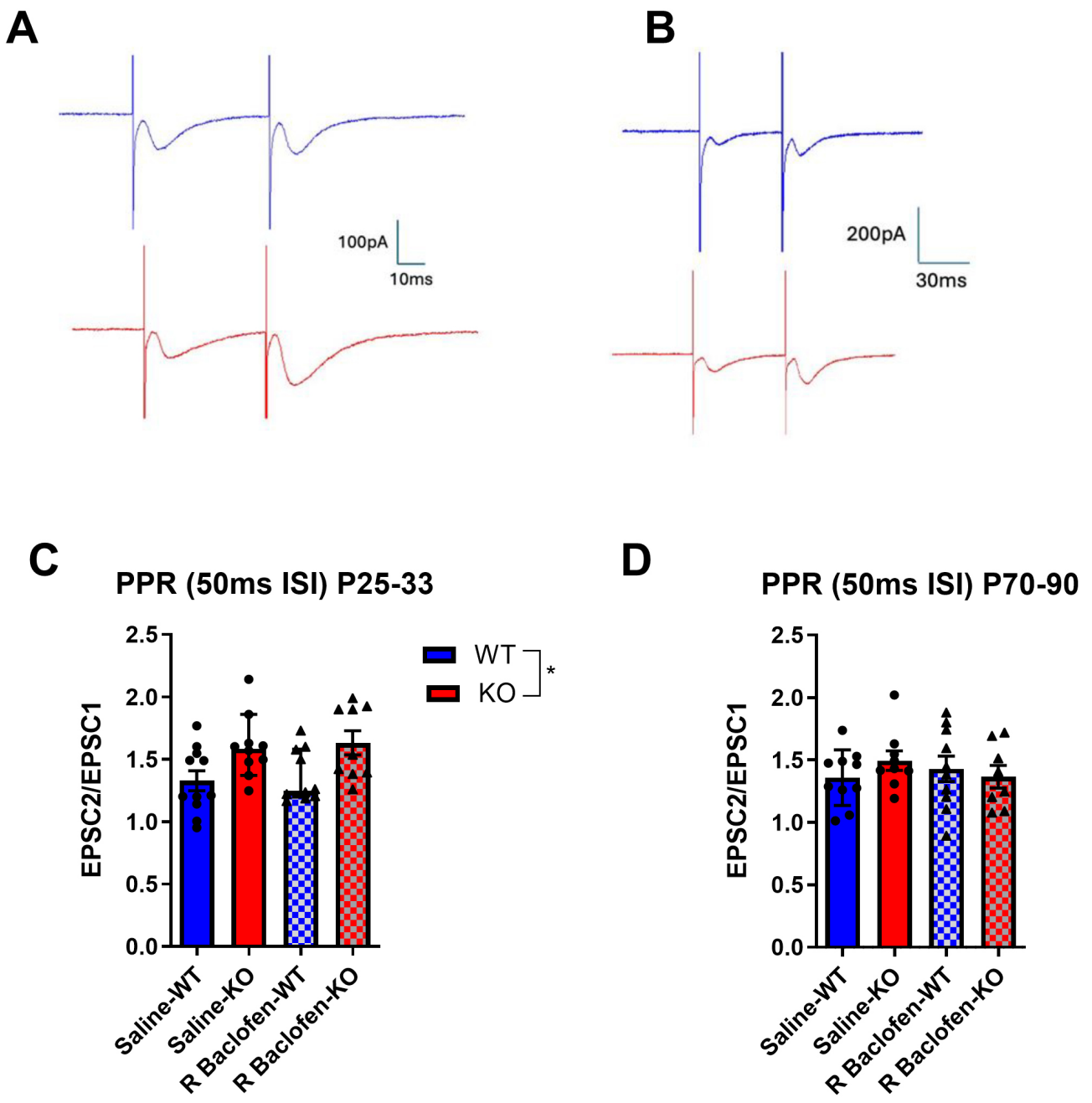

Fig. 6. Paired pulse ratios of synaptic potentials in auditory cortical neurons. (A) Sample recordings of excitatory postsynaptic currents (EPSCs) used to calculate paired pulse ratios in slices of juvenile and of (B) adult animals. (C) Paired Pulse Ratios in juvenile and in (D) adult animals. Animal/cell counts–P25–33: saline-WT: N = 5/n = 11, saline-KO: N = 6/n = 10, rbac-WT: N = 4/n = 10, rbac-KO: N = 4/n = 9; P70–90: saline WT: N = 3/n = 10, saline-KO: N = 3/n = 9, rbac-WT: N = 4/n = 10, rbac-KO: N = 5/n = 8. Graphs show means ± SEM. Statistical comparisons were performed using a linear mixed-effects model. Asterisks indicate significant differences, $*p < 0.05$.

4.3 Effects of Early Treatment With R-Baclofen on Firing Rates

Firing frequencies in response to depolarizing current were altered in KO neurons: while initially lower in the juvenile stage, firing rates in adult KO neurons trended toward increased responsivity at low levels of depolarizing current injection, but as depolarizing current intensity increased, firing rates in KO neurons did not hold up as well as in WT neurons and became lower than in WT. This lower slope of the I/O function in adult cortical auditory neurons has also been observed in a previous study using *in vitro* electrophysiological recordings with step current stimulation [48]. Interestingly, R-baclofen treatment had a significant effect on juvenile KO neurons, reversing

the slightly lower firing rates. By adulthood, the impact of treatment persisted as neurons from KO animals treated with R-baclofen no longer significantly differed in F-I slope from WTs, and although firing remained somewhat reduced at higher depolarizations, there was an overall improvement in neuronal responsivity. $GABA_B$ receptor activation could influence the firing rates through a variety of processes, potentially impacting plasticity at the axon initial segments (AIS), ion channel composition, or homeostatic synaptic plasticity [49,50,51,52,53]. Given that *Cntnap2* loss disrupts the organization of voltage-gated potassium channels at juxtaparanodes and the AIS during development [3,54], KO neurons may be particularly vulnerable to these types of perturbations, which may also explain why R-baclofen treatment did not impact firing profiles in WTs at either age. Future research could directly test these possibilities by introducing synaptic blockers during recordings to isolate intrinsic properties, voltage-clamp pharmacology to evaluate specific K^+ currents, or structural/molecular analyses of AIS organization and ion channel expression/localization. As well, it is important to consider that since we did find a genotypic difference in RMP at P25–33, there is potential that this could impact firing frequencies, as RMP in KO animals would be further from the threshold and thus reduce firing frequencies. However, since we did not find any genotypic difference in rheobase or firing thresholds, it is unlikely that RMP alone could explain differences in cell excitability and responsivity. The more prominent difference in F-I slopes and normalization of RMP alterations during adulthood supports this further.

4.4 Effects of Early Treatment With R-Baclofen on Synaptic Signaling

KO neurons exhibited increased frequency of sPSCs in addition to higher PPRs relative to WT neurons. Since increased frequency of sPSCs indicates greater synaptic activity, but PPR facilitation indicates lower release probability at each individual synapse, this could be interpreted as an increased number of synaptic inputs to *Cntnap2* KO neurons, with reduced individual release probabilities. This corresponds well with findings in the auditory brainstem of adult *Cntnap2* KO animals, where a higher number of neurons was reported to be activated in response to a startle sound, indicating higher connectivity [55]. The reduced release probability might compensate for higher connectivity to maintain synaptic homeostasis [56]. However, since synaptic blockers were not used to separate excitatory and inhibitory components or to isolate miniature PSCs, it is not possible to determine if hyperconnectivity is definitively supported. Though it is plausible, there could be other contributions to the observed increase in synaptic input, such as increased presynaptic firing. Further, similar to the intrinsic membrane properties, any differences in synaptic activity due to R-baclofen treatment were normalized by adulthood.

4.5 Integrating Changes due to R-Baclofen Treatment

In juveniles, firing profiles in neurons from saline-treated KO animals displayed a trend toward hypo-excitability relative to saline-WTs, whereas R-baclofen treatment significantly shifted KO firing patterns closer to saline-WT levels. However, saline-KOs also exhibited increased sPSC frequency, and R-baclofen further increased sPSC frequency, suggesting either increased synaptic connectivity or upregulated synaptic input. Thus, careful interpretation of the "normalization" of firing frequency in KOs is warranted. R-baclofen did not necessarily reverse the KO effects and restore WT-like physiology, but instead, intrinsic neuronal hypo-excitability seemed to have been counteracted through exacerbated synaptic input. Future studies using synaptic receptor antagonists (e.g., AMPA/kainite receptor antagonist CNQX, $GABA_A$ receptor antagonist PTX) during recordings would help isolate intrinsic excitability by removing ongoing synaptic input, thereby clarifying whether the observed changes in neuronal excitability are driven by cell-autonomous mechanisms or are masked and/or shaped by alterations in synaptic drive.

Even so, compensatory effects like these could potentially contribute to known paradoxical effects of GABA agonists observed in some patients, including those with ASD [57,58]. For example, benzodiazepines modulate $GABA_A$ receptors to enhance inhibitory tone and acutely reduce anxiety. However, it is well documented that chronic exposure to such compounds can induce rebound anxiety or even worsening of baseline anxiety following discontinuation/dose reduction [59]. Neurobiologically, chronic $GABA_A$ activation can lead to reduced receptor sensitivity, altered subunit composition, upregulation of excitatory transmission, and a net shift in E/I balance toward excitation [60,61]. These adaptive changes may be conceptually consistent with the cellular alterations observed following early-life R-baclofen exposure in the present study. Future work should therefore aim to elucidate $GABA_B$ receptor-specific adaptations following prolonged treatment across development.

Our results show that early developmental perturbations may exert lasting consequences on cortical circuit maturation, ultimately producing altered excitability phenotypes in adults. A similar trajectory has been reported in pyramidal neurons of the *Dlx1* knockout mouse, a model for post-developmental loss of interneurons. In this case, loss of inhibitory interneurons induced reductions in excitatory synaptic drive and intrinsic excitability around 30 days of age, which normalized across development, while altered firing network dynamics emerged later on [62]. Together, these findings suggest that apparent normalization of neuronal properties may mask complex, developmentally emergent changes in excitability, thereby providing a plausible mechanistic framework for the developmental shift in excitability alterations observed in the *Cntnap2* KO rat.

Overall, these results highlight both the risks and the potential of early-life exposure to R-baclofen. In *Cntnap2* KO rats, early R-baclofen treatment largely reversed *Cntnap2*-related changes in firing frequencies, but it also exacerbated changes in synaptic input in an age-dependent manner. Moreover, in juvenile WT neurons, R-baclofen transiently altered the intrinsic excitability by depolarizing resting membrane potentials and raising firing thresholds. Although these effects resolved by adulthood, they highlight that treatment with a $GABA_B$ agonist is capable of disrupting intrinsic neuronal properties, including in healthy neurons. This has important translational implications on the therapeutic use of R-baclofen in pediatric patients, as this treatment has not only the potential to change the developmental trajectory of the brain, but also can disrupt maturation of intrinsic excitability in non-affected neurons. This is especially critical when considering the implications of treatment during developmental periods when ion channel expression and AIS organization are still being refined [63]. Our findings highlight the importance of proper developmental timing and thorough diagnosis of potential underlying genetic and physiological causes before considering a $GABA_B$ agonist-based therapy. Future work should aim to determine the behavioural manifestations of early-life treatment with R-baclofen to assess how electrophysiological changes may translate into functional outcomes.

4.6 Limitations

While the present findings provide important insights into therapeutic intervention in *Cntnap2*-related ASD, several methodological constraints limit their interpretation. First, sex was not included as a factor in our analyses in order to preserve statistical power. In addition, sex distribution was not balanced between groups, further limiting the ability to accurately assess sex as a potential modifying factor. Although statistical power considerations were prioritized, we acknowledge that sexual dimorphism in ASD, as well as in GABAergic signaling, is well established. This is also relevant to the *Cntnap2* KO model, in which sex-dependent differences have been reported at both the behavioural and cellular levels. Future studies should therefore strongly prioritize appropriate experimental design and powering to assess sex as a biological variable, in order to better evaluate the efficacy and safety of R-baclofen treatment. Moreover, although acute slice electrophysiology provides high-resolution insights into cellular and synaptic function, there are inherent limitations in its translatability to clinical outcomes. During tissue preparation, acute slicing preserves only local microcircuits while severing long-range inputs and outputs. As such, although we observed changes in neuronal properties presently, these findings do not necessarily map onto behaviour, as clinical outcomes arise from integrated and distributed networks. Furthermore, brain slice preparations may lack intact neuromodulatory tone, limiting the expression of state-dependent dynamics such as oscillations and network transitions, and may introduce sampling bias toward neurons that are more resilient to the slicing procedure.

5. Conclusions

In conclusion, we've shown that *Cntnap2* loss produces age-dependent alterations in neuronal function, with juvenile neurons exhibiting changes in resting membrane potential, cell capacitance, firing thresholds, and synaptic input, and adult neurons displaying pronounced shifts in firing dynamics, including an indication of a different gain pattern. Early-life exposure to R-baclofen partially normalized the alterations in firing frequency in juvenile and adult KO neurons, yet induced complex, sometimes unwanted age-specific effects on intrinsic and synaptic properties. When translating these findings into the clinic, one also has to keep in mind that only a fraction of autistic patients have a loss in *Cntnap2* function or in a related protein. Nevertheless, our findings provide some understanding of the long-term consequences of early pharmacological treatment and the challenges of developing therapeutic interventions in neurodevelopmental disorders, particularly in autism, where the large heterogeneity of underlying biological causes almost prohibits a "one-size-fits-all" approach to treatment.

Availability of Data and Materials

All data reported in this paper will be shared by the corresponding author upon request.

Author Contributions

HP and SS designed the research study. HP performed the research. SS provided help and technical advice. HP analyzed the data. HP wrote the first draft of the manuscript. SS edited the manuscript. Both authors read and approved the final manuscript. Both authors have participated sufficiently in the work and agreed to be accountable for all aspects of the work.

Ethics Approval and Consent to Participate

All animal procedures were approved by the Animal Care Committee of the University of Western Ontario (AUP: 2025-0087 and AUP 2024-0002) and followed the rules and regulations of the Canadian Council on Animal Care. All animal procedures followed the ARRIVE 2.0 guidelines (**Supplementary Material**).

Acknowledgment

Thanks to all manuscript reviewers for their constructive feedback.

Funding

This study was supported by the Natural Sciences and Engineering Council Canada (NSERC 04472-2018 PIN)

and the Canadian Institutes of Health Research (CIHR PJT168866).

Conflicts of Interest

The authors declare no conflicts of interest.

Supplementary Material

Supplementary material associated with this article can be found, in the online version, at https://doi.org/10.31083/JIN52072.

References

[1] Alarcón M, Abrahams BS, Stone JL, Duvall JA, Perederiy JV, Bomar JM, et al. Linkage, association, and gene-expression analyses identify CNTNAP2 as an autism-susceptibility gene. American Journal of Human Genetics. 2008; 82: 150–159. https://doi.org/10.1016/j.ajhg.2007.09.005.

[2] Bakkaloglu B, O'Roak BJ, Louvi A, Gupta AR, Abelson JF, Morgan TM, et al. Molecular cytogenetic analysis and resequencing of contactin associated protein-like 2 in autism spectrum disorders. American Journal of Human Genetics. 2008; 82: 165–173. https://doi.org/10.1016/j.ajhg.2007.09.017.

[3] Poliak S, Salomon D, Elhanany H, Sabanay H, Kiernan B, Pevny L, et al. Juxtaparanodal clustering of Shaker-like K+ channels in myelinated axons depends on Caspr2 and TAG-1. The Journal of Cell Biology. 2003; 162: 1149–1160. https://doi.org/10.1083/jcb.200305018.

[4] Gdalyahu A, Lazaro M, Penagarikano O, Golshani P, Trachtenberg JT, Geschwind DH. The Autism Related Protein Contactin-Associated Protein-Like 2 (CNTNAP2) Stabilizes New Spines: An In Vivo Mouse Study. PloS One. 2015; 10: e0125633. https://doi.org/10.1371/journal.pone.0125633.

[5] Poot M. Connecting the CNTNAP2 Networks with Neurodevelopmental Disorders. Molecular Syndromology. 2015; 6: 7–22. https://doi.org/10.1159/000371594.

[6] Poot M. Intragenic CNTNAP2 Deletions: A Bridge Too Far? Molecular Syndromology. 2017; 8: 118–130. https://doi.org/10.1159/000456021.

[7] Gordon A, Salomon D, Barak N, Pen Y, Tsoory M, Kimchi T, et al. Expression of Cntnap2 (Caspr2) in multiple levels of sensory systems. Molecular and Cellular Neurosciences. 2016; 70: 42–53. https://doi.org/10.1016/j.mcn.2015.11.012.

[8] Peñagarikano O, Geschwind DH. What does CNTNAP2 reveal about autism spectrum disorder? Trends in Molecular Medicine. 2012; 18: 156–163. https://doi.org/10.1016/j.molmed.2012.01.003.

[9] Strauss KA, Puffenberger EG, Huentelman MJ, Gottlieb S, Dobrin SE, Parod JM, et al. Recessive symptomatic focal epilepsy and mutant contactin-associated protein-like 2. The New England Journal of Medicine. 2006; 354: 1370–1377. https://doi.org/10.1056/NEJMoa052773.

[10] Arking DE, Cutler DJ, Brune CW, Teslovich TM, West K, Ikeda M, et al. A common genetic variant in the neurexin superfamily member CNTNAP2 increases familial risk of autism. American Journal of Human Genetics. 2008; 82: 160–164. https://doi.org/10.1016/j.ajhg.2007.09.015.

[11] Peñagarikano O, Abrahams BS, Herman EI, Winden KD, Gdalyahu A, Dong H, et al. Absence of CNTNAP2 leads to epilepsy, neuronal migration abnormalities, and core autism-related deficits. Cell. 2011; 147: 235–246. https://doi.org/10.1016/j.cell.2011.08.040.

[12] Scott KE, Schormans AL, Pacoli KY, De Oliveira C, Allman BL, Schmid S. Altered Auditory Processing, Filtering, and Reactivity in the Cntnap2 Knock-Out Rat Model for Neurodevelopmental Disorders. The Journal of Neuroscience : the Official Journal of the Society for Neuroscience. 2018; 38: 8588–8604. https://doi.org/10.1523/JNEUROSCI.0759-18.2018.

[13] Scott KE, Kazazian K, Mann RS, Möhrle D, Schormans AL, Schmid S, et al. Loss of Cntnap2 in the Rat Causes Autism-Related Alterations in Social Interactions, Stereotypic Behavior, and Sensory Processing. Autism Research : Official Journal of the International Society for Autism Research. 2020; 13: 1698–1717. https://doi.org/10.1002/aur.2364.

[14] Varea O, Martin-de-Saavedra MD, Kopeikina KJ, Schürmann B, Fleming HJ, Fawcett-Patel JM, et al. Synaptic abnormalities and cytoplasmic glutamate receptor aggregates in contactin associated protein-like 2/Caspr2 knockout neurons. Proceedings of the National Academy of Sciences of the United States of America. 2015; 112: 6176–6181. https://doi.org/10.1073/pnas.1423205112.

[15] Selimbeyoglu A, Kim CK, Inoue M, Lee SY, Hong ASO, Kauvar I, et al. Modulation of prefrontal cortex excitation/inhibition balance rescues social behavior in CNTNAP2-deficient mice. Science Translational Medicine. 2017; 9: eaah6733. https://doi.org/10.1126/scitranslmed.aah6733.

[16] Gao F, Qi L, Yang Z, Yang T, Zhang Y, Xu H, et al. Impaired GABA Neural Circuits Are Critical for Fragile X Syndrome. Neural Plasticity. 2018; 2018: 8423420. https://doi.org/10.1155/2018/8423420.

[17] Vogt D, Cho KKA, Shelton SM, Paul A, Huang ZJ, Sohal VS, et al. Mouse Cntnap2 and Human CNTNAP2 ASD Alleles Cell Autonomously Regulate PV+ Cortical Interneurons. Cerebral Cortex (New York, N.Y. : 1991). 2018; 28: 3868–3879. https://doi.org/10.1093/cercor/bhx248.

[18] Lazaro MT, Taxidis J, Shuman T, Bachmutsky I, Ikrar T, Santos R, et al. Reduced Prefrontal Synaptic Connectivity and Disturbed Oscillatory Population Dynamics in the CNTNAP2 Model of Autism. Cell Reports. 2019; 27: 2567–2578.e6. https://doi.org/10.1016/j.celrep.2019.05.006.

[19] Cording KR, Tu EM, Wang H, Agopyan-Miu AHCW, Bateup HS. Cntnap2 loss drives striatal neuron hyperexcitability and behavioral inflexibility. elife. 2025; 13: RP100162. https://doi.org/10.7554/eLife.100162.

[20] Mann RS, Allman BL, Schmid S. Developmental changes in electrophysiological properties of auditory cortical neurons in the Cntnap2 knockout rat. Journal of Neurophysiology. 2023; 129: 937–947. https://doi.org/10.1152/jn.00029.2022.

[21] Rubenstein JLR, Merzenich MM. Model of autism: increased ratio of excitation/inhibition in key neural systems. Genes, Brain, and Behavior. 2003; 2: 255–267. https://doi.org/10.1034/j.1601-183x.2003.00037.x.

[22] Wang P, Sun J. A comprehensive review of GABA in autism spectrum disorders: associations, mechanisms, and therapeutic implications. Frontiers in Psychiatry. 2025; 16: 1587432. https://doi.org/10.3389/fpsyt.2025.1587432.

[23] Purcell AE, Jeon OH, Zimmerman AW, Blue ME, Pevsner J. Postmortem brain abnormalities of the glutamate neurotransmitter system in autism. Neurology. 2001; 57: 1618–1628. https://doi.org/10.1212/wnl.57.9.1618.

[24] Brown MS, Singel D, Hepburn S, Rojas DC. Increased glutamate concentration in the auditory cortex of persons with autism and first-degree relatives: a (1)H-MRS study. Autism Research : Official Journal of the International Society for Autism Research. 2013; 6: 1–10. https://doi.org/10.1002/aur.1260.

[25] Cai J, Ding L, Zhang JS, Xue J, Wang LZ. Elevated plasma levels of glutamate in children with autism spectrum disorders. Neuroreport. 2016; 27: 272–276. https://doi.org/10.1097/WNR.0000000000000532.

[26] Fatemi SH, Halt AR, Stary JM, Kanodia R, Schulz SC, Realmuto GR. Glutamic acid decarboxylase 65 and 67 kDa pro-

teins are reduced in autistic parietal and cerebellar cortices. Biological Psychiatry. 2002; 52: 805–810. https://doi.org/10.1016/s0006-3223(02)01430-0.

[27] Oblak AL, Gibbs TT, Blatt GJ. Decreased GABA(B) receptors in the cingulate cortex and fusiform gyrus in autism. Journal of Neurochemistry. 2010; 114: 1414–1423. https://doi.org/10.1111/j.1471-4159.2010.06858.x.

[28] Zikopoulos B, Barbas H. Altered neural connectivity in excitatory and inhibitory cortical circuits in autism. Frontiers in Human Neuroscience. 2013; 7: 609. https://doi.org/10.3389/fnhum.2013.00609.

[29] Möhrle D, Wang W, Whitehead SN, Schmid S. GABAB Receptor Agonist R-Baclofen Reverses Altered Auditory Reactivity and Filtering in the Cntnap2 Knock-Out Rat. Frontiers in Integrative Neuroscience. 2021; 15: 710593. https://doi.org/10.3389/fnint.2021.710593.

[30] Kaupmann K, Malitschek B, Schuler V, Heid J, Froestl W, Beck P, et al. GABA(B)-receptor subtypes assemble into functional heteromeric complexes. Nature. 1998; 396: 683–687. https://doi.org/10.1038/25360.

[31] Silverman JL, Pride MC, Hayes JE, Puhger KR, Butler-Struben HM, Baker S, et al. GABAB Receptor Agonist R-Baclofen Reverses Social Deficits and Reduces Repetitive Behavior in Two Mouse Models of Autism. Neuropsychopharmacology : Official Publication of the American College of Neuropsychopharmacology. 2015; 40: 2228–2239. https://doi.org/10.1038/npp.2015.66.

[32] Sinclair D, Oranje B, Razak KA, Siegel SJ, Schmid S. Sensory processing in autism spectrum disorders and Fragile X syndrome-From the clinic to animal models. Neuroscience and Biobehavioral Reviews. 2017; 76: 235–253. https://doi.org/10.1016/j.neubiorev.2016.05.029.

[33] Sharghi S, Flunkert S, Daurer M, Rabl R, Chagnaud BP, Leopoldo M, et al. Evaluating the effect of R-Baclofen and LP-211 on autistic behavior of the BTBR and Fmr1-KO mouse models. Frontiers in Neuroscience. 2023; 17: 1087788. https://doi.org/10.3389/fnins.2023.1087788.

[34] Alruwaili NS, Al-Kuraishy HM, Fahad EH, Al-Gareeb AI, Alhelfawi S, Mustafa AM, et al. Unravelling GABA Dysfunction in Autism: Pathophysiological Insights and Emerging Treatments. International Journal of Developmental Neuroscience : the Official Journal of the International Society for Developmental Neuroscience. 2026; 86: e70103. https://doi.org/10.1002/jdn.70103.

[35] Parellada M, San José Cáceres A, Delorme R, Moscoso A, Moreno C, Calvo R, et al. Efficacy, safety, and tolerability of arbaclofen in Autistic children and adolescents, the AIMS-2-TRIALS-CT1: a randomized, double-blind, placebo-controlled phase II trial. EClinicalMedicine. 2026; 92: 103760. https://doi.org/10.1016/j.eclinm.2026.103760.

[36] Geal-Dor M, Freeman S, Li G, Sohmer H. Development of hearing in neonatal rats: air and bone conducted ABR thresholds. Hearing Research. 1993; 69: 236–242. https://doi.org/10.1016/0378-5955(93)90113-f.

[37] Berardi N, Pizzorusso T, Maffei L. Critical periods during sensory development. Current Opinion in Neurobiology. 2000; 10: 138–145. https://doi.org/10.1016/s0959-4388(99)00047-1.

[38] de Villers-Sidani E, Chang EF, Bao S, Merzenich MM. Critical period window for spectral tuning defined in the primary auditory cortex (A1) in the rat. The Journal of Neuroscience : the Official Journal of the Society for Neuroscience. 2007; 27: 180–189. https://doi.org/10.1523/JNEUROSCI.3227-06.2007.

[39] Takesian AE, Bogart LJ, Lichtman JW, Hensch TK. Inhibitory circuit gating of auditory critical-period plasticity. Nature Neuroscience. 2018; 21: 218–227. https://doi.org/10.1038/s41593-017-0064-2.

[40] Zaman T, De Oliveira C, Smoka M, Narla C, Poulter MO, Schmid S. BK Channels Mediate Synaptic Plasticity Underlying Habituation in Rats. The Journal of Neuroscience : the Official Journal of the Society for Neuroscience. 2017; 37: 4540–4551. https://doi.org/10.1523/JNEUROSCI.3699-16.2017.

[41] Dolphin AC, Scott RH. Inhibition of calcium currents in cultured rat dorsal root ganglion neurones by (-)-baclofen. British Journal of Pharmacology. 1986; 88: 213–220. https://doi.org/10.1111/j.1476-5381.1986.tb09489.x.

[42] Scott RH, Dolphin AC. Regulation of calcium currents by a GTP analogue: potentiation of (-)-baclofen-mediated inhibition. Neuroscience Letters. 1986; 69: 59–64. https://doi.org/10.1016/0304-3940(86)90414-3.

[43] Gähwiler BH, Brown DA. GABAB-receptor-activated K+ current in voltage-clamped CA3 pyramidal cells in hippocampal cultures. Proceedings of the National Academy of Sciences of the United States of America. 1985; 82: 1558–1562. https://doi.org/10.1073/pnas.82.5.1558.

[44] Browning KN, Travagli RA. Mechanism of action of baclofen in rat dorsal motor nucleus of the vagus. American Journal of Physiology. Gastrointestinal and Liver Physiology. 2001; 280: G1106–13. https://doi.org/10.1152/ajpgi.2001.280.6.G1106.

[45] Bushart DD, Huang H, Man LJ, Morrison LM, Shakkottai VG. A Chlorzoxazone-Baclofen Combination Improves Cerebellar Impairment in Spinocerebellar Ataxia Type 1. Movement Disorders : Official Journal of the Movement Disorder Society. 2021; 36: 622–631. https://doi.org/10.1002/mds.28355.

[46] Zheng A, Schmid S. A review of the neural basis underlying the acoustic startle response with a focus on recent developments in mammals. Neuroscience and Biobehavioral Reviews. 2023; 148: 105129. https://doi.org/10.1016/j.neubiorev.2023.105129.

[47] Cisneros-Franco JM, Voss P, Thomas ME, de Villers-Sidani E. Critical periods of brain development. Handbook of Clinical Neurology. 2020; 173: 75–88. https://doi.org/10.1016/B978-0-444-64150-2.00009-5.

[48] Scott KE, Mann RS, Schormans AL, Schmid S, Allman BL. Hyperexcitable and immature-like neuronal activity in the auditory cortex of adult rats lacking the language-linked CNTNAP2 gene. Cerebral Cortex (New York, N.Y. : 1991). 2022; 32: 4797–4817. https://doi.org/10.1093/cercor/bhab517.

[49] Grubb MS, Burrone J. Building and maintaining the axon initial segment. Current Opinion in Neurobiology. 2010; 20: 481–488. https://doi.org/10.1016/j.conb.2010.04.012.

[50] Kuba H. Plasticity at the axon initial segment. Communicative & Integrative Biology. 2010; 3: 597–598. https://doi.org/10.4161/cib.3.6.13242.

[51] Kole MHP, Stuart GJ. Signal processing in the axon initial segment. Neuron. 2012; 73: 235–247. https://doi.org/10.1016/j.neuron.2012.01.007.

[52] Turrigiano G. Homeostatic synaptic plasticity: local and global mechanisms for stabilizing neuronal function. Cold Spring Harbor Perspectives in Biology. 2012; 4: a005736. https://doi.org/10.1101/cshperspect.a005736.

[53] Heine M, Ciuraszkiewicz A, Voigt A, Heck J, Bikbaev A. Surface dynamics of voltage-gated ion channels. Channels (Austin, Tex.). 2016; 10: 267–281. https://doi.org/10.1080/19336950.2016.1153210.

[54] Pinatel D, Hivert B, Saint-Martin M, Noraz N, Savvaki M, Karagogeos D, et al. The Kv1-associated molecules TAG-1 and Caspr2 are selectively targeted to the axon initial segment in hippocampal neurons. Journal of Cell Science. 2017; 130: 2209–2220. https://doi.org/10.1242/jcs.202267.

[55] Zheng A, Scott KE, Schormans AL, Mann R, Allman BL, Schmid S. Differences in Startle and Prepulse Inhibition in Contactin-associated Protein-like 2 Knock-out Rats are Associated with Sex-specific Alterations in Brainstem Neural Activity.

Neuroscience. 2023; 513: 96–110. https://doi.org/10.1016/j.neuroscience.2023.01.020.

[56] Turrigiano GG, Leslie KR, Desai NS, Rutherford LC, Nelson SB. Activity-dependent scaling of quantal amplitude in neocortical neurons. Nature. 1998; 391: 892–896. https://doi.org/10.1038/36103.

[57] Marrosu F, Marrosu G, Rachel MG, Biggio G. Paradoxical reactions elicited by diazepam in children with classic autism. Functional Neurology. 1987; 2: 355–361.

[58] Bruining H, Passtoors L, Goriounova N, Jansen F, Hakvoort B, de Jonge M, et al. Paradoxical Benzodiazepine Response: A Rationale for Bumetanide in Neurodevelopmental Disorders? Pediatrics. 2015; 136: e539–43. https://doi.org/10.1542/peds.2014-4133.

[59] Pétursson H. The benzodiazepine withdrawal syndrome. Addiction (Abingdon, England). 1994; 89: 1455–1459. https://doi.org/10.1111/j.1360-0443.1994.tb03743.x.

[60] Miller LG, Greenblatt DJ, Roy RB, Summer WR, Shader RI. Chronic benzodiazepine administration. II. Discontinuation syndrome is associated with upregulation of gamma-aminobutyric acidA receptor complex binding and function. The Journal of Pharmacology and Experimental Therapeutics. 1988; 246: 177–182.

[61] Xiang K, Tietz EI. Chronic benzodiazepine-induced reduction in GABA(A) receptor-mediated synaptic currents in hippocampal CA1 pyramidal neurons prevented by prior nimodipine injection. Neuroscience. 2008; 157: 153–163. https://doi.org/10.1016/j.neuroscience.2008.08.049.

[62] Howard MA, Rubenstein JLR, Baraban SC. Bidirectional homeostatic plasticity induced by interneuron cell death and transplantation in vivo. Proceedings of the National Academy of Sciences of the United States of America. 2014; 111: 492–497. https://doi.org/10.1073/pnas.1307784111.

[63] Gutzmann A, Ergül N, Grossmann R, Schultz C, Wahle P, Engelhardt M. A period of structural plasticity at the axon initial segment in developing visual cortex. Frontiers in Neuroanatomy. 2014; 8: 11. https://doi.org/10.3389/fnana.2014.00011.